

HAPTEN-LINKED CONFORMATIONAL EQUILIBRIA IN IMMUNOGLOBULINS XRPC-24 AND J-539 OBSERVED BY CHEMICAL RELAXATION

S. VUK-PAVLOVIĆ, Y. BLATT, C. P. J. GLAUDEMANS, D. LANCET, AND
I. PECHT, *Department of Chemical Immunology, The Weizmann Institute
of Science, Rehovot, Israel, and Laboratory of Chemistry, National
Institute of Arthritis, Metabolism and Digestive Diseases, National
Institutes of Health, Bethesda, Maryland 20014 U.S.A.*

ABSTRACT The interaction of oligogalactan haptens with the murine myeloma proteins XRPC-24 and J-539 has been investigated by the fluorescence temperature-jump method. The relaxation spectrum is composed of two processes, the faster representing hapten association and the slower a protein isomerization. In both cases the concentration dependence of relaxation times and amplitudes was consistent with the general mechanism formulated by Lancet and Pecht (1976, *Proc. Natl. Acad. Sci. U.S.A.* **73**:3549), in which the equilibrium between two conformations of the protein is shifted by hapten binding. The intact proteins and their Fab fragment had identical kinetic behavior, indicating that the conformational changes are located in the Fab region. Temperature dependence analysis for protein J-539 permitted the calculation of activation parameters and led to a consistent energy profile for all the elementary steps. The conformational states are separated by large activation barriers, but have similar free energies. The results suggest that hapten-induced conformational changes in immunoglobulins are more general phenomena than was previously thought.

INTRODUCTION

Immunoglobulins recognize antigens and bind them to the variable portions in their Fab parts by multiple noncovalent interactions. The antigen-antibody complexes thus formed are capable of activating various macromolecular and cellular functions related to the immune response. The triggering of these events involves sites on the Fc region of the immunoglobulin away from the antigen-binding site. The molecular mechanism of this signal transmission has not yet been clearly resolved, and several models, not mutually exclusive, have been proposed for it (1). In one of these, the allosteric model, it is assumed that antigen (or hapten) binding will impose structural changes in the hapten binding domain (Fv) or possibly in the whole Fab, which may then propagate to the Fc (2).

Dr. Vuk-Pavlović's permanent address is: Institute of Immunology, 41000 Zagreb, Yugoslavia. Address correspondence to Dr. Pecht, Department of Structural Biology, Sherman Fairchild Building, Stanford University School of Medicine, Stanford, Calif. 94305.

Recently we have reported kinetic evidence for an isomerization step in the homogeneous immunoglobulin MOPC 460 which is linked to the binding of hapten (3). In the present paper we similarly analyze the elementary steps in the interaction of the homogeneous immunoglobulins secreted by murine plasmacytomas J-539 and XRPC-24 with their specific (1 → 6)- β -D-oligogalactan haptens (4). The observed chemical relaxation spectra are shown to be as expected for an allosteric monomer, where two interconvertible conformations of the hapten-binding domains exist, and hapten shifts the equilibrium between them towards the better binding one. The present findings are therefore consistent with an allosteric model for antibody action. They provide a detailed dynamic and energetic picture of the processes involved in such a possible mechanism.

MATERIALS AND METHODS

Mildly reduced and alkylated homogeneous murine plasmacytoma proteins J-539 and XRPC-24 (X-24), their Fab fragments, and the haptens (1-6)- β -D-galactotriose (Gal₃) and (1-6)- β -D-galactotetraose (Gal₄) were prepared as previously described (4). In all experiments phosphate-buffered saline (PBS; 0.01 M phosphate, 0.15 M NaCl, pH 7.0) was used.

Kinetic measurements used a temperature jump apparatus, as described by Rigler et al. (5), operating in the fluorescence mode. Capacitor discharge of 20 kV raised the temperature by 5.2° from 20.0 ± 0.1° or 30.0 ± 1°C. The analog signal was digitized by a Biomation 802 transient recorder (Biomation, Cupertino, Calif.). The sum of at least five relaxation curves was analyzed by a computer program using a modified Marquardt routine (6). The program yielded the relaxation times and the corresponding amplitudes. These amplitudes were normalized by a generalized version of the formula used by Lancet and Pecht (3): $A = (\Delta F_{\text{obs}}/F) / (1 + \Delta f_{\text{max}} \theta)$, where A is the normalized amplitude, ΔF_{obs} and F are the observed changes in fluorescence and the total fluorescence after the temperature jump both in the same arbitrary units, Δf_{max} is the maximal fractional fluorescence change at full saturation (negative for quenching and positive for enhancement), and θ is the fractional saturation of the protein at the particular hapten concentration. The experimental concentration dependence of the relaxation times and amplitudes was fitted to expressions according to Lancet and Pecht (3), using the algorithm of Powell (7).

RESULTS AND INTERPRETATION

The relaxation spectrum for both proteins XRPC-24 and J-539 with Gal₃ consists of a biexponential decay. The two relaxation times are observed throughout the hapten concentration range and are well separated. No relaxation process was observed for any of the reactants alone. In the case of XRPC-24, the analysis was problematic due to the interference of the cooling of the sample with the slower relaxation component. The amplitudes were more sensitive to such deviations, and therefore only a limited analysis of relaxation times is presented here. In the case of protein J-539 the slower relaxation was completed within 1 s, and the data allowed full analysis, which resulted in a complete and self-consistent picture of the binding and conformational equilibria.

The concentration dependences of the fast ($1/\tau_f$) and slow ($1/\tau_s$) relaxation rates for proteins XRPC-24 and J-539 binding Gal₃ at 25°C are shown in Figs. 1 and 2, re-

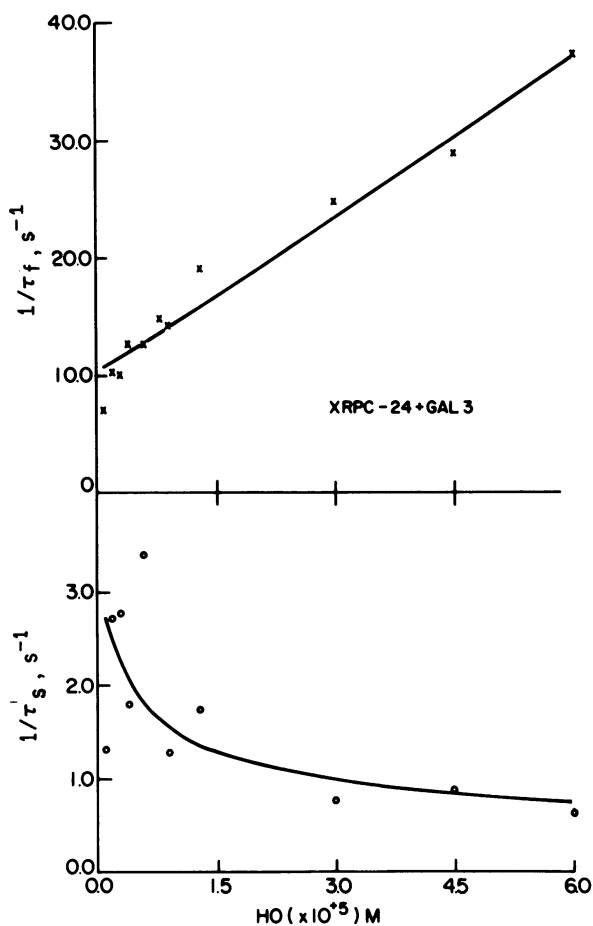
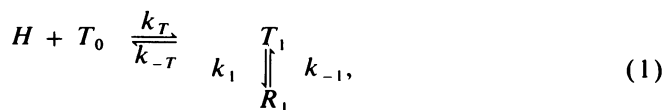
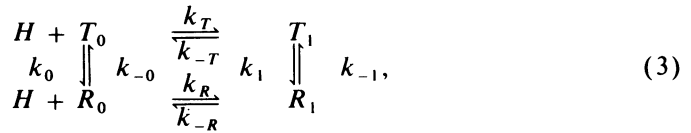
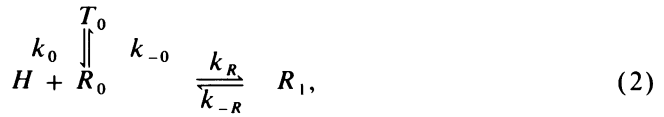


FIGURE 1 The dependence of fast (x) and slow (o) reciprocal relaxation times of XRPC-24 on total Gal₃ concentration at 25°C. Intact protein concentration was 9.52×10^{-7} M sites. The lines were calculated by using the best fit parameters for mechanism 3, as listed in Table I. Individual values (in all figures) are $\pm 5\%$.

spectively. It can be seen that for both proteins $1/\tau_f$ increases linearly, while $1/\tau_s$ levels off with increasing hapten concentration. Such behavior indicates the presence of a bimolecular association together with a slower monomolecular step, which we attribute to protein isomerization.

Lancet and Pecht (3) have amply discussed the mechanisms which may be considered when evaluating antibody-hapten interactions, for which also a monomolecular slow step is observed. These mechanisms are (in the standard nomenclature of Monod et al. [8]):





where the isomerizations occur in the hapten-antibody complex (mechanism 1), in the free antibody (mechanism 2), or in both (mechanism 3). For a comprehensive table listing the detailed kinetic and thermodynamic features of these mechanisms, the reader is referred to ref. 3.

Kinetics of Gal₃ Binding to XRPC-24

The concentration dependence plots in Fig. 1 represent experiments with intact protein XRPC-24, but the Fab fragment gave practically identical results. A qualitative in-

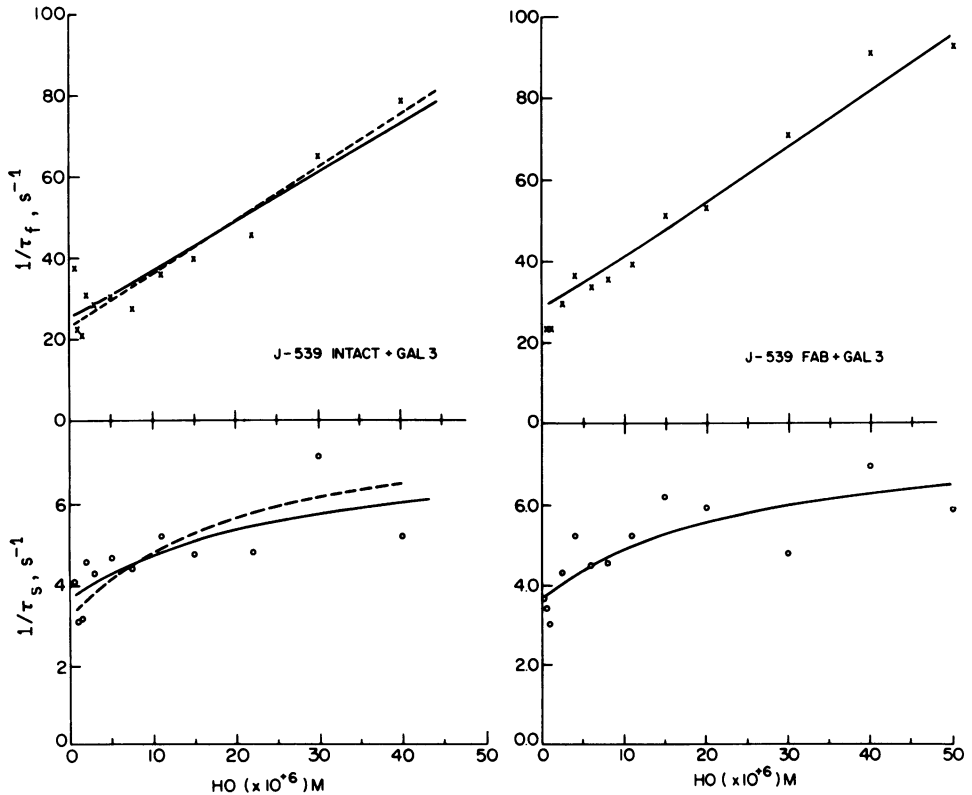


FIGURE 2 The dependence of fast (x) and slow (o) reciprocal relaxation times of J-539 on total Gal₃ concentration at 25°C. Left: intact protein, 9.52×10^{-7} M sites. Right: Fab fragment, 1.33×10^{-6} M sites. The broken and solid lines were calculated by using the best fit parameters for mechanism 1 and 3, respectively.

TABLE I
KINETIC PARAMETERS FOR THE REACTION BETWEEN INTACT XRPC-24 AND
GAL₃ AT 25°C

<i>i</i>	K_i	k_i	k_{-i}	ΔG_i
		s^{-1}	s^{-1}	<i>kcal/mol</i>
<i>T</i>	4.5×10^4	4.5×10^5	10.0	-6.32
<i>R</i>	2.7×10^5	—	—	-7.38
0	0.5	1.05	2.09	0.41
1	3.0	0.3	0.1	-0.65
Overall	1.2×10^5			-6.90

spection of these plots leads to the rejection of mechanisms 1 and 2. This may be seen as follows: $1/\tau_s$ decreases to a plateau, behavior consistent with mechanism 2, but not with 1. On the other hand, the slope over intercept of the $1/\tau_f$ line yields a rough estimate of the binding constant for the fast association. This is found to be $k_{\text{ass}} = 5 \times 10^4 \text{ M}^{-1}$, smaller than the known overall association constant $K = 1.75 \times 10^5 \text{ M}^{-1}$ for XRPC-24 Fab (4). Such relation may be obtained for mechanism 1, but not for 2. Only mechanism 3 is compatible with both these observations simultaneously.

The lines in Fig. 1 represent the best fit of the data to Eqs. 4 and 5 below. The corresponding best fit parameters are listed in Table I. We have also performed experiments with Gal₄ haptens. The data obtained were identical to those with Gal₃ within the experimental error and, therefore, are not presented here. However, this finding supports the notion of Jolley et al., who found that the fourth galactose in the oligomer does not contribute much to the total binding energy (9).

Kinetics of Gal₃ Binding to J-539

For the protein J-539 the relaxation times (τ_f , τ_s) as well as the fast (A_f) and slow (A_s) relaxation amplitudes were analyzed in detail. The data for the intact protein and Fab at 25°C are depicted in Figs. 2 and 3. Here, the relation between K_{ass} and overall equilibrium constant, K , is as found for XRPC-24 ($K_{\text{ass}} = 5.8 \times 10^4 \text{ M}^{-1}$, $K = 1.5 \times 10^5 \text{ M}^{-1}$ [4]), while the behavior of the slow time is different: $1/\tau_s$ increases to a plateau. This means that mechanism 1 may be used to account for the relaxation phenomena. Analysis in terms of this mechanism revealed fairly good agreement with the data (dashed lines in Figs. 2 and 3) for all four relaxation quantities (τ_f , τ_s , A_f , A_s) yielding the following parameter values: $k_T = 1.31 \times 10^6 \text{ M}^{-1} \text{ s}^{-1}$, $k_{-T} = 23.4 \text{ s}^{-1}$, $K_T = 5.77 \times 10^4 \text{ M}^{-1}$, $k_1 = 4.82 \text{ s}^{-1}$, $k_{-1} = 3.01 \text{ s}^{-1}$, $K_1 = 1.68$ with the overall equilibrium constant fixed at the value $K = 1.5 \times 10^5 \text{ M}^{-1}$ (4).

Mechanism 1 was shown to be a special limiting case of mechanism 3 (3). A system that fits mechanism 1 may in principle also be described in terms of the thermodynamically general mechanism 3. Since two other immunoglobulin-hapten equilibria (MOPC-460 and XRPC-24) were shown to fit only the latter mechanism, it forms the only basis for comparison of all three systems. Furthermore, only mechanism 3 provides a full insight into the energy and activation attributes of hapten-induced con-

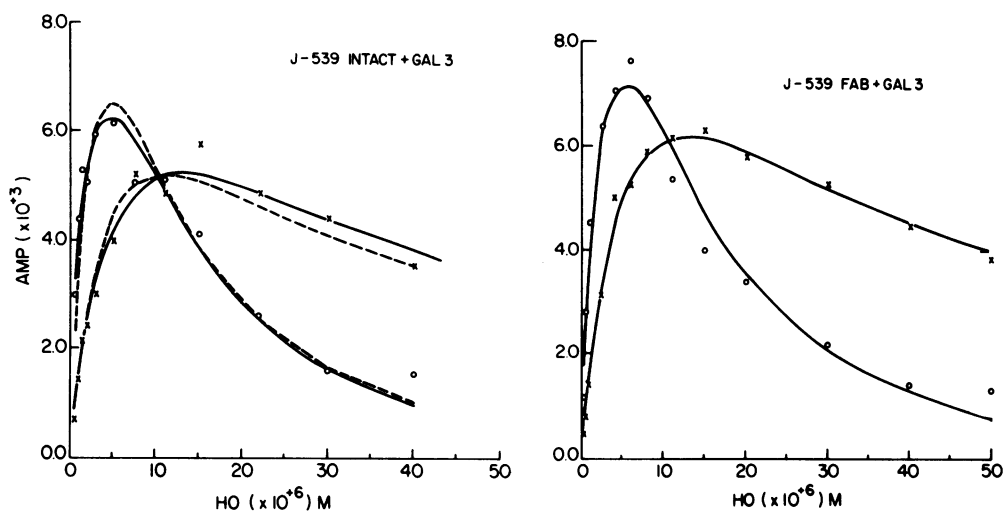


FIGURE 3 The dependence of fast (x) and slow (o) amplitude of J-539 intact (left) and Fab (right) on total Gal₃ concentration. The points are $\Delta F_{\text{obs}}/F$ (see Materials and Methods) and the normalization is done on the fitted lines. Other details are the same as in Fig. 2.

formational changes (see below). We therefore chose to analyze the relaxation data presented above also in terms of mechanism 3.

For this mechanism one expects three relaxation times. When the associations are much faster than the isomerizations, two of these represent the *T* and *R* association steps and one the isomerization steps (10). For both XRPC-24 and J-539 (as also found in the case of MOPC-460, ref. 3) one observes only two relaxation times. An attempt to fit the relaxation spectra to a sum of three exponents gave a very large scatter in the concentration dependence, implying that such procedure was chemically meaningless and that only two relaxation times really occur. We explain this discrepancy assuming that the spectral change of one of the steps is zero. The concentration dependences of τ_f and A_f are found by the fitting procedure to be compatible only with those of a *T* association, and a fit with $\Delta f_R = 0$ indeed yields consistent results as seen below.

The concentration dependences were fitted to the following equations derived according to Castellán (10) and Jovin (11):

$$1/\tau_f = k_T \cdot g_{11} \cdot T_0 \cdot H, \quad (4)$$

$$1/\tau_s = |g_3| \cdot (k_1 \cdot T_1 + k_0 \cdot T_0) / |g_2|, \quad (5)$$

$$A_f = \Delta H_T \cdot \Delta f_T \cdot \Delta T / (g_{11} \cdot A_0 \cdot R \cdot T^2), \quad (6)$$

$$A_s = |g_2| \cdot (Q_{13} \cdot \Delta f_T + Q_{23} \cdot \Delta f_R + \Delta f_0) \cdot (Q_{13} \cdot \Delta H_T + Q_{23} \cdot \Delta H_R + \Delta H_0) \cdot \Delta T / (|g_3| \cdot R \cdot T^2 \cdot A_0), \quad (7)$$

where Δf_i and ΔH_i are the normalized fluorescence change and standard enthalpy change of step *i*, A_0 is the total protein concentration, and $Q_{13} = (g_{12} \cdot g_{23} - g_{13} \cdot g_{22}) /$

$|g_2|$, $Q_{23} = (g_{12} \cdot g_{13} - g_{11} \cdot g_{23}) / |g_2|$. g_{ij} and $|g_i|$ are an element and a principal partial determinant of the Castellan g -matrix (10). These equations are identical to those used by Lancet and Pecht (3): both there and here the Castellan form was used in the computer fit, being concise and easy to formulate. The equations may then be transformed by somewhat tedious algebraic manipulations into the explicit form given by Lancet and Pecht.

The best-fit lines for J-539 (intact and Fab at 25°C) are shown in Fig. 2 (full line curves), and the corresponding parameters are given in Table II. It is clearly seen that the intact protein and the Fab fragment give very similar relaxation patterns and parameters. The following points should be stressed in the context of these fits: (a) As mentioned above, only the T association gives rise to an observable relaxation process. Eq. 4 is derived by assuming that this process is the fastest in the system. We also attempted a fit assuming that the R association is faster, and that the T association is coupled to it, but a worse fit was obtained. (b) The information on the parameters of the unobservable R association is obtained through the fit of the slow time and amplitude (Eqs. 6 and 7). (c) The overall Δf was fixed in the fitting procedure to the value measured previously (4). K and ΔH on the other hand, were left as free parameters and their values in Table II represent the best fit. No independent information is available for ΔH , while K agrees fairly well with $K = 1.5 \times 10^5 \text{ M}^{-1}$ previously reported (4).

Experiments were also performed at 15° and 35°C. At 15°C the relaxation was so slow that numerical evaluation was unreliable. A good fit was obtained for the data at 35°C with parameters as listed in Table II. From the change of k_i with temperature,

TABLE II
KINETIC AND THERMODYNAMIC PARAMETERS FOR THE REACTION BETWEEN INTACT OR Fab FRAGMENT OF J-539 AND GAL_3 AT 25 AND 35°C ACCORDING TO MECHANISM 3

i	T	K_i	k_i	k_{-i}	ΔF_i	ΔH_i	ΔG_i	ΔS_i	
	°C		s^{-1}	s^{-1}		kcal/mol		cal/mol · °	
T	Intact	25	4.96×10^4	1.23×10^6	24.8	0.2	-12.8	-6.38	-21.5
	Fab	25	4.96×10^4	1.36×10^6	27.4	0.25	-12.5	-6.38	-20.5
	Fab	35	2.95×10^4	2.17×10^6	73.3	0.27	-12.7	-6.07	-22.2
R	Intact	25	1.96×10^5	—	—	0.0*	-10.6	-7.19	-11.4
	Fab	25	1.96×10^5	—	—	0.0*	-10.7	-7.19	-11.8
	Fab	35	1.15×10^5	—	—	0.0*	-10.0	-6.88	-10.5
0	Intact	25	0.93	1.77	1.91	0.3	-0.63	0.043	-3.56
	Fab	25	0.93	1.77	1.91	0.45	-0.26	0.043	-1.02
	Fab	35	0.9	5.16	5.74	0.37	-0.27	0.062	-1.02
1	Intact	25	3.67	5.72	1.56	0.009	0.53	-0.77	4.36
	Fab	25	3.67	6.09	1.66	-0.09	-0.48	-0.77	0.97
	Fab	35	3.5	20.6	5.88	0.64	-0.31	-0.74	1.44
Overall	Intact	25	1.2×10^5	—	—	0.196	-11.3	-6.9	-14.8
	Fab	25	1.2×10^5	—	—	0.255	-10.7	-6.9	-12.7
	Fab	35	7×10^4	—	—	0.255	-10.7	-6.58	-13.8

Error $\pm 20\%$.

*Assumption.

TABLE III
ACTIVATION PARAMETERS FOR THE REACTION BETWEEN PROTEIN J-539 Fab
AND GAL₃ ACCORDING TO MECHANISM 3, CALCULATED FROM THE KINETIC
PARAMETERS AT 25 AND 35°C.

<i>i</i>	<i>T</i>	<i>-T</i>	0	-0	1	-1
$\Delta G_i^\ddagger, \text{kcal/mol}$	9.05	15.4	17.0	17.0	16.3	17.1
$\Delta H_i^\ddagger, \text{kcal/mol}$	7.88	17.3	18.8	19.4	21.5	22.4
$\Delta S_i^\ddagger, \text{cal/mol} \cdot ^\circ$	-3.92	6.28	5.89	8.06	17.4	17.8
$\Delta G_i^\ddagger - \Delta G_{-i}^\ddagger, \text{kcal/mol}$		-6.38		0.04		-0.78
$\Delta H_i^\ddagger - \Delta H_{-i}^\ddagger, \text{kcal/mol}$		-9.42		-0.59		-0.87
$\Delta S_i^\ddagger - \Delta S_{-i}^\ddagger, \text{cal/mol} \cdot ^\circ$		-10.2		-2.17		-0.46

the activation parameters were calculated by the Eyring equation (12). The resultant values are given in Table III. The difference $\Delta H_i^\ddagger - \Delta H_{-i}^\ddagger$ is the overall enthalpy change in the step, and it is obtained here in an independent way. Comparison to the values obtained from the amplitude analysis (Table II) reveals satisfactory agreement, and this is true also for ΔG^\ddagger and ΔS^\ddagger . Thus, the internal consistency of the analysis performed here is clearly brought out.

DISCUSSION

The present kinetic study provides a detailed insight into the dynamics and energetics of hapten-induced conformational transitions in two sugar-binding immunoglobulins. For both XRPC-24 and J-539 the results are consistent with the "allosteric monomer" model (mechanism 3) where two conformational states of the protein, *T* and *R*, bind the hapten differently ($K_R > K_T$). $\Delta(\Delta G) = \Delta G_R - \Delta G_T$ serves as the driving force for the shift in the conformational equilibrium, as it is also equal to $\Delta G_1 - \Delta G_0$, and therefore

$$\Delta G_1 = \Delta G_0 + \Delta(\Delta G). \quad (8)$$

For both XRPC-24 and J-539 ΔG_0 is found to be small and positive, (0.41 and 0.06 kcal/mol, respectively), implying *T*₀ is more stable and that the two states differ only slightly in their free energy. The value of $\Delta(\Delta G)$, although not very large (-1.1 and -0.8 kcal/mol, respectively), is sufficient to make ΔG_1 negative in both cases, so that *R*₁ becomes the predominant conformation. The extent of the hapten-induced shift in the conformational equilibrium is given by K_1/K_0 ($= K_R/K_T = 1/c$ in the Monod et al. model, ref. 8), and is 4.0 and 6.0 for J-539 and XRPC-24. This is somewhat smaller than 11.4 found for MOPC 460 (3).

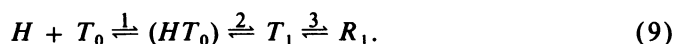
The rate constants for the conformational processes are found to be in the range of 1-10 s⁻¹ at 25°, so that $\Delta G^\ddagger = 16-17$ kcal/mol. The *k* values are 3-4-fold higher at 35°, due to the high positive ΔH^\ddagger for the isomerizations (18-22 kcal/mol). The low rates and high activation parameters most probably reflect the participation of a significant portion of the Fab in the conformational transition, i.e., many interactions are

disrupted to attain the transition state. The positive ΔS^\ddagger , on the other hand, implies that entropically favorable processes are involved in its formation.

It thus appears that, although the two conformations have almost identical G and H values (Table II), they are separated by a significant energetic barrier. This barrier is somewhat higher here than that found for MOPC 460, where isomerization rate constants are $10\text{--}100\text{ s}^{-1}$, and $\Delta H^\ddagger = 10\text{ kcal/mol}$ (3, 13).

The values of k_{on} for the protein-oligosaccharide associations are found here to be two orders of magnitude lower than those for nitroaromatic-binding immunoglobulins (13), and comparable to those found for other sugar-binding proteins (13, 14). This may stem from the necessity to overcome the flexibility of the ligand (reflected in $\Delta S^\ddagger_7 < 0$) and/or from the need to disrupt and form many hydrogen bonds upon association, expressed in the large positive ΔH^\ddagger_7 (see ref. 13 for a discussion of this point).

For another sugar-binding immunoglobulin, Maeda et al. (14) suggest that such a slow association step includes a monomolecular (possibly conformational) rearrangement of the hapten-immunoglobulin complex. If this mechanism, originally proposed by Haselkorn et al. (15) to describe any hapten-antibody association, holds also in our case, then the full binding scheme (written for simplicity in terms of our mechanism 1) should be:



In this scheme, step 1 represents the formation of the encounter complex (13) or a process of labile association (14). Step 2 may involve hydrogen-bond exchange and/or fast conformational rearrangements of both the ligand and protein contact residues, which do not give rise to a resolvable reaction step. Step 1 and 2 together result in a single fast relaxation step (cf. ref. 13). Step 3 represents those conformational changes in the protein which involve higher energetic barriers, and therefore give rise to a distinct slow relaxation time.

The present study extends the kinetic evidence for hapten-induced conformational changes in immunoglobulins. Thus, such phenomena are not restricted only to rare cases or to a particular type of hapten. Our data suggest that a large portion of the Fab is involved in the kinetically observed conformational transition, but that it does not depend on the Fc. It is however possible that high molecular weight antigens, having a larger $\Delta(\Delta G)$, are able to shift the conformational equilibrium more significantly and by a mechanism such as that proposed by Huber et al. (2) will lead to changes also in the Fc. In addition, the observed conformational changes may be related to the attainment of optimal antibody-antigen complementarity, and may thus be relevant to the question of antibody diversity.

S.V.-P. gratefully acknowledges a long-term fellowship from the European Molecular Biology Organization.

Received for publication 10 December 1977.

REFERENCES

1. METZGER, H. 1974. Effect of antigen binding on the properties of antibody. *Adv. Immunol.* **18**:169.
2. HUBER, R., J. DEISENHOFER, P. M. COLMAN, M. MATSUSHIMA, and W. PALM. 1976. Crystallographic structure studies of an IgG molecule and an Fc fragment. *Nature (Lond.)* **264**:415.
- PECHT, I. 1976. Recognition and allostery in the mechanism of antibody action. *Collog. Ges. Biol. Chem. Mosbach.* **27**:41.
3. LANCET, D., and I. PECHT. 1976. Kinetic evidence for hapten induced conformational transition in immunoglobulin MOPC 460. *Proc. Natl. Acad. Sci. U.S.A.* **73**:3549.
4. JOLLY, M. E., S. RUDIKOFF, M. POTTER, and C. P. J. GLAUDEMANS. 1973. Spectral changes on binding of oligosaccharides to murine immunoglobulin A myeloma proteins. *Biochemistry.* **12**:3039.
5. RIGLER, R., C. R. RABL, and T. M. JOVIN. 1974. A temperature-jump apparatus for fluorescence measurements. *Rev. Sci. Instrum.* **45**:580.
6. FLETCHER, R. 1971. In Harwell Subroutine Library, Atomic Energy Research Establishment, Harwell, U.K. (Subroutine VB01A).
7. POWELL, M. J. D. 1971. In Harwell Subroutine Library, Atomic Energy Research Establishment, Harwell, U.K. (Subroutine VA04A).
8. MONOD, J., J. WYMAN, and J. P. CHANGEUX. 1965. On the nature of allosteric transitions: a plausible model. *J. Mol. Biol.* **12**:88.
9. JOLLEY, M. E., C. P. J. GLAUDEMANS, S. RUDIKOFF, and M. POTTER. 1974. Structural requirements for the binding of derivatives of D-galactose to two homogeneous murine immunoglobulins. *Biochemistry.* **13**:3179.
10. CASTELLAN, G. W. 1963. Calculation of the spectrum of chemical relaxation times for a general reaction mechanism. *Ber. Bunsenges. Phys. Chem.* **67**:898.
11. JOVIN, T. 1975. Fluorimetric kinetic techniques: chemical relaxation and stopped flow. In *Biochemical Fluorescence Concepts*. R. F. CHEN, and H. EDELHOCH, editors. Marcel Dekker, Inc., New York. Vol. 1, 305.
12. GLASSTONE, S., K. J. LAIDLER, and H. EYRING. 1941. The theory of rate processes. McGraw-Hill Book Company, New York. 14.
13. PECHT, I., and D. LANCET. 1977. Kinetics of antibody-hapten interaction. In *Chemical Relaxation in Molecular Biology*. I. Pecht and R. Rigler, Editors. Springer-Verlag, Berlin. 306.
14. MAEDA, H., A. SCHMIDT-KESSEN, J. ENGEL, and J. C. JATON. 1977. Kinetics of binding of oligosaccharides to a homogeneous pneumococcal antibody: dependence on antigen chain length suggests a labile intermediate complex. *Biochemistry.* **16**:4086.
15. HASELKORN, D., S. FRIEDMAN, D. GIVOL, and I. PECHT. 1974. Kinetic mapping of the antibody combining site by chemical relaxation spectrometry. *Biochemistry.* **13**:2210.

DISCUSSION

SCHECHTER: The first two questions were submitted by a referee: What are the best numerical procedures now available for the analysis of chemical relaxation data of the type presented here? Within what confidence limit can the relaxation decay law be determined and what are some of the main artifacts to be avoided in studies of this type?

PECHT: The analysis includes two major consecutive steps: (a) Analysis of the relaxation curves and evaluation of relaxation times and amplitudes (and base lines): Routinely, a sum of six or more relaxation curves has been analyzed. In principle any least-squares fit procedure may be used. We found that the modified algorithm of Marquardt is particularly effective (cf. ref. 6 for the subroutine). This subroutine requires the derivative of the exponential function with respect to the parameters, but the first guesses supplied to the program need not be very accurate. (b) Analysis of the concentration dependence of the relaxation times and amplitude: Here the functions are often more complex, and analytical derivations are not always convenient. Therefore